Journal of Physics: Conference Series **381** (2012) 012093 doi:10.1088/1742-6596/381/1/012093

N/Z effects on dynamics of Ca+Ca collisions at 25 MeV/nucleon

I. Lombardo[1,7], L. Acosta[1], C. Agodi[1], F. Amorini[1], A. Anzalone[1], L. Auditore[4], I. Berceanu[9], G. Cardella[2], S. Cavallaro[1,3], M.B. Chatterjee[8], E. DeFilippo[2], E. Geraci[2,3], G. Giuliani[2,3], L. Grassi[2,3], J. Han[1], E. LaGuidara[3,5], G. Lanzalone[1,6], D. Loria[4], C. Maiolino[1], A. Pagano[2], M. Papa[2], S. Pirrone[2], G. Politi[2,3], F. Porto[1,3], F. Rizzo[1,3], P. Russotto[1,3], A. Trifirò[4], M. Trimarchi[4], G. Verde[2], M. Vigilante[6]

[1] INFN - Laboratori Nazionali del Sud, Via S. Sofia, Catania, Italy
[2] INFN - Sezione di Catania, Via S. Sofia, Catania, Italy
[3] Dipartimento di Fisica e Astronomia, Università di Catania, Via S. Sofia, Catania, Italy
[4] Dipartimento di Fisica, Università di Messina, and INFN-Gr.Coll. Messina, Italy
[5] Facoltà di Ingegneria ed Architettura, Università Kore di Enna, Enna, Italy
[6] Dipartimento di Scienze Fisiche, Università di Napoli Federico II, and INFN-Sez. Napoli, Italy
[7] Centro Siciliano di Fisica Nucleare e Struttura della Materia, Catania, Italy
[8] Saha Institute of Nuclear Physics, Kolkata, India
[9] Institute for Physics and Nuclear Engineering, Bucharest, Romania

E-mail: ilombardo@lns.infn.it

Abstract. Semi-central events of collisions $^{40,48}Ca + ^{40,48}Ca$ at 25 MeV/nucleon have been investigated by means of the Chimera multi-detector array. We find that the competition between evaporation residue and two or more fragment emission is regulated in a strong way by the neutron to proton ratio of the total reaction system. Comparisons of experimental data and Constrained Molecular Dynamics model calculations allow to obtain information about the behavior of the symmetry energy of the nuclear Equation of State.

1. Introduction

In the last years, the study of effects due to the neutron richness on nuclear reactions in the Fermi energy domain has attracted increasingly the interest of both experimental and theoretical communities [1, 2, 3]. The comparison of experimental data with theoretical calculations concerning various aspects of nuclear dynamics has allowed to obtain increasingly precise information about the behavior of the symmetry energy in the nuclear Equation of State [4].

One of the observables, that has been shown to be sensitive to the symmetry energy, is the competition between various reaction mechanisms that can be observed in medium mass nuclear reactions near 30 MeV/nucleon [2]. For example, it has been pointed out theoretically that the interplay between symmetry energy and Coulomb effects can influence the fate of very excited intermediate systems produced at semi-central impact parameter [5, 6]. In this case, the reaction cross section is distributed between evaporation residues emission (produced mainly by means of

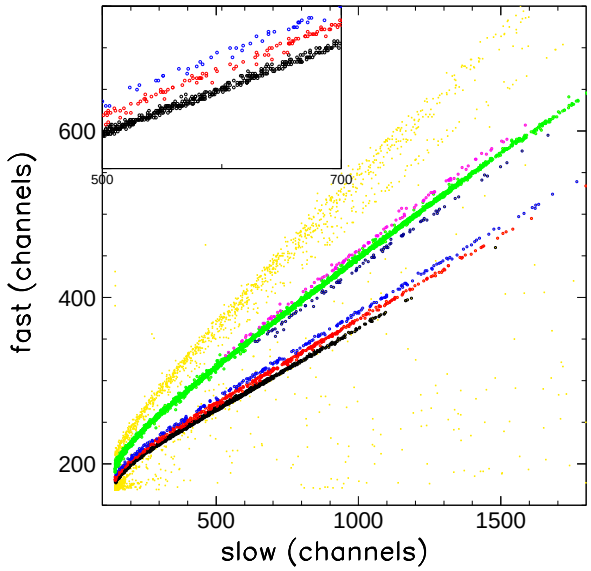

Figure 1. Fast-slow correlation obtained from the CsI(Tl) light output in the $^{40}Ca + ^{48}Ca$ collision at 25 MeV/nucleon. Black points: protons. Red points: deuterons. Blue points: tritons. α particles are in green, while ^{3}He and ^{6}He are in dark blue and violet, respectively. In the insert, a zoomed vision of hydrogen isotopes is shown.

incomplete fusion mechanisms [7]) and other, more complex, phenomena where the production of two or more fragments is observed [8].

To investigate these topics, we performed the set of nuclear reactions $^{40,48}Ca + ^{40,48}Ca$ at 25 MeV/nucleon. In this way, we are able to obtain various medium mass nuclear systems with the largest possible range of neutron to proton ratios (N/Z) available by using stable beams (from the $N = Z$ symmetric system $^{40}Ca + ^{40}Ca$ up to the very neutron rich reaction $^{48}Ca + ^{48}Ca$, having $N = 1.4Z$). To check if the observed effects are not biased by the (slightly) different masses of entrance channels, we performed also the collision $^{40}Ca + ^{46}Ti$ at 25 MeV/nucleon; it has a total mass and a mass asymmetry very similar to that of $^{40}Ca + ^{48}Ca$, but with marked difference in the neutron to proton ratio of entrance channels (N/Z=1.05 versus N/Z=1.2). From the analysis of semi-peripheral events of reactions, we find that the emission of evaporation residues is highly sensitive to the neutron richness of the total system formed [9, 10, 11]. The comparison of experimental data with Constrained Molecular Dynamics model [12, 13] calculations allows moreover to get information about the stiffness of the symmetry energy at near-saturation densities.

2. Experimental apparatus

We used beams of ^{40}Ca and ^{48}Ca accelerated by the Super-Conductive Cyclotron of INFN-Laboratori Nazionali del Sud at 25 MeV/nucleon. Isotopically enriched ^{40}Ca (1.24 mg/cm^2 thick) and ^{48}Ca (2.7 mg/cm^2 thick) self-supporting targets have been used. Reaction products have been detected by means of the 4π multi-detector Chimera [14]; it is constituted by 1192 Si-CsI(Tl) counter telescopes, covering about 94% of the solid angle. The nominal thickness of silicon detectors is $300\mu m$, while CsI(Tl) thickness varies as a function of the polar angle from 3 cm (backward angles) up to 12 cm (forward angles).

Fragments that punch through the silicon detectors can be identified in charge with good resolution; they can be also isotopically resolved up to $Z \approx 10$ or more [15]. Light charged

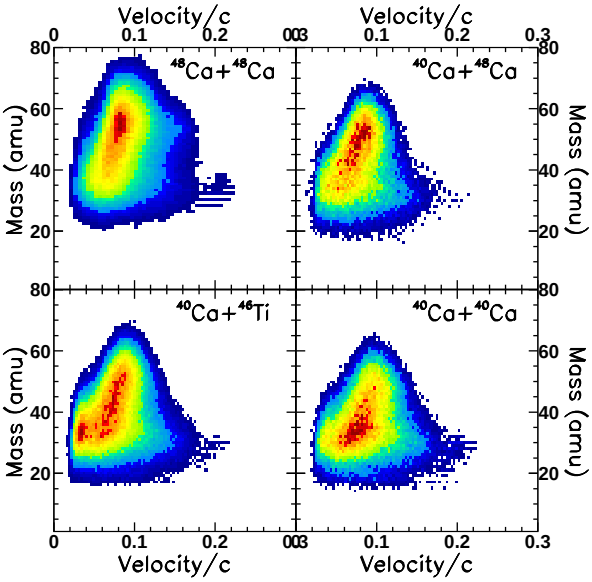

Figure 2. Mass-velocity correlations (m_1, v_1) of the largest fragment emitted in semi-central events of reactions $^{40}Ca+^{40}Ca$, $^{40}Ca+^{46}Ti$, $^{40}Ca+^{48}Ca$ and $^{48}Ca+^{48}Ca$ at 25 MeV/nucleon.

particles (as $p, d, t, ^3He, \alpha$) can be isotopically resolved also by performing fast-slow analysis of CsI(Tl) light output [16]. As an example, a typical fast-slow matrix obtained for a Chimera CsI(Tl) is shown in Figure 1; hydrogens and helions can be resolved in mass with a good quality. Further details about this array and its detection capabilities can be found in Refs. [14, 15, 16]. The mass of fragments stopped in silicon detectors can be estimated by performing time of flight and kinetic energy measurements. Time resolution typically achieved is $\approx 800ps$; it is due mostly to time characteristics of the beam. The obtained mass resolution ($\frac{\Delta m}{m}$) is around 5% [9] for nuclei having mass $A \approx 50$.

We analyzed only well reconstructed events; i.e. events where the total detected charge Z_{tot} was between 80% and 100% of the total charge. This selection allow to discard spurious events on oxygen contaminant in the target and pile-up phenomena. To improve the completeness of selected events, we require moreover the detection of at least 60% of the entrance parallel momentum. Quasi-elastic events were removed during the experiment by requiring the detection of at least 3 charged particles.

3. Evaporation residue emission

To select semi-central events of reaction we imposed constraint on charged particle multiplicity, as suggested by Ref. [17]. We selected moreover those events where the presence of a fast quasi-projectile nucleus, typical of massive transfer phenomena, is clearly seen [18]. To do this, we require that the second or the third largest fragment emitted in each event of reaction has a velocity larger than 1.3 times the center of mass velocity ($v_{cm} \approx 0.11c$).

We plot on figure 2 the correlation of mass (m_1) and velocity (v_1) of the largest fragment emitted in the selected semi-central events of reactions $^{40}Ca+^{40,48}Ca$, ^{46}Ti and $^{48}Ca+^{48}Ca$ (apart from slight kinematical difference, the scatter plot of $^{48}Ca+^{40}Ca$ events is quite similar to that of $^{40}Ca+^{48}Ca$ case). Even if the overall shapes of all correlations are similar, the enhanced emission of evaporation residues for the $^{48}Ca+^{48}Ca$ reaction is quite evident. At variance, by decreasing the N/Z of entrance channels, the bump associated to evaporation residue emission ($m_1 \approx 50 - 55uma$) is more and more softened and, at the same time, events where the largest

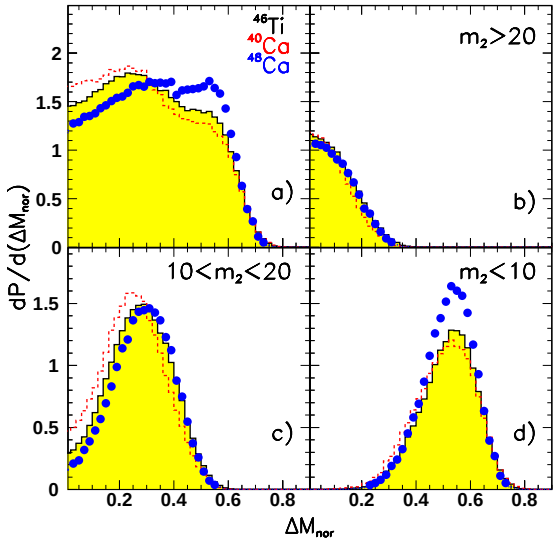

Figure 3. Experimental ΔM_{nor} distribution shown as a function of the different targets used in the experiment. (a) No selection on m_2. (b) Selection $m_2 \geq 20$. (c) Selection $10 \leq m_2 \leq 20$. (d) Selection $m_2 \leq 10$. Blue dots: $^{40}Ca + ^{48}Ca$. Red dashed histogram: $^{40}Ca + ^{40}Ca$. Shadow area histogram: $^{40}Ca + ^{46}Ti$.

fragment emitted has a mass lower than the projectile one become increasingly important [11]. It seems therefore that the balance between production of evaporation residues and the presence of other phenomena is strongly affected by the N/Z degree of freedom; in particular, nuclear reactions characterized by a high N/Z value of entrance channels show a larger probability of producing evaporation residues by means of incomplete fusion [9, 10, 11]. The investigation of $^{40}Ca + ^{46}Ti$ allows to conclude that the observed N/Z effects are not biased by the total mass and mass asymmetry of the entrance channel [9].

To investigate in more detail dynamical effects involving the emission of evaporation residues in the selected events of reaction, we plot on Figure 3 the difference between the masses of the two largest fragments emitted normalized to the total mass of the systems: $\Delta M_{nor} = \frac{m_1 - m_2}{m_{tot}}$, for the $^{40}Ca + ^{40,48}Ca, ^{46}Ti$ reactions. In order to exclude target-like contributions biased by differences in the target thickness, we take into account only fragments having velocities larger than 0.04c. The use of the ΔM_{nor} quantity allows to minimize effects due to the small mass difference between the entrance channels and enhances isospin asymmetry effects [9].

By looking at Figure 3.a, for the case of $^{40}Ca + ^{48}Ca$ reactions, an enhancement in the region $\Delta M_{nor} \approx 0.5$ is quite evident; it corresponds to the emission of an evaporation residue. On the other hand, in the $N = Z$ symmetric reaction $^{40}Ca + ^{40}Ca$, the distribution is clearly pushed to lower ΔM_{nor} values. $^{40}Ca + ^{46}Ti$, having an intermediate neutron to proton ratio, shows an intermediate behavior.

The differences between the three studied systems can be disentangled by looking at the ΔM_{nor} distribution as a function of different selections on m_2, the mass of the second largest fragment (Figure 3b,c,d). The constraint $m_2 \leq 10$ amu enlightens in a good way incomplete fusion events. In this case ΔM_{nor} distributions peak around 0.55; this region corresponds clearly to the emission of evaporation residues. The probability of populating this region of the ΔM_{nor} distribution is higher for $^{40}Ca + ^{48}Ca$ reaction as compared to the other two systems (as observed in Figure 3d). On the contrary, the constraints $m_2 \geq 20$ and $10 \leq m_2 \leq 20$ are associated to

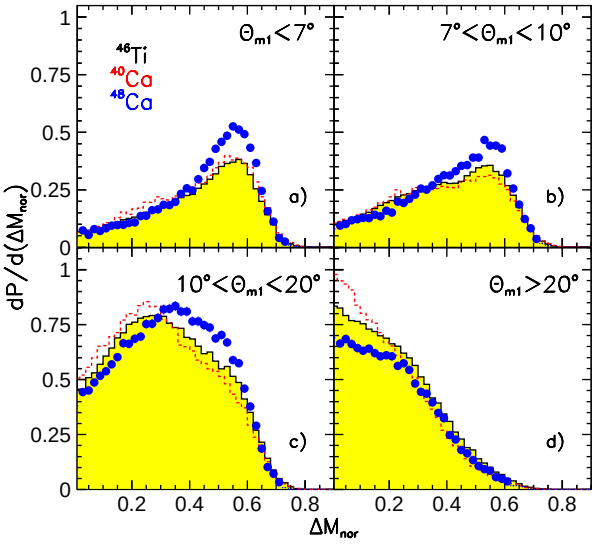

Figure 4. Experimental ΔM_{nor} distributions shown as a function of the different targets used in reactions $^{40}Ca + ^{40,48}Ca, ^{46}Ti$ at 25 MeV/nucleon. (a) The largest fragment is emitted at a polar angle $\Theta_{m1} \leq 7°$. (b) The largest fragment is emitted at a polar angle $7° \leq \Theta_{m1} \leq 10°$. (c) The largest fragment is emitted at a polar angle $10° \leq \Theta_{m1} \leq 20°$. (d) The largest fragment is emitted at a polar angle $\Theta_{m1} \geq 20°$.

binary-like, fusion-fission and multi-fragmentation phenomena; in fact the ΔM_{nor} distributions are pushed to lower values [9].

It is also interesting to investigate the ΔM_{nor} distributions as a function of the emission angle of the largest fragment (Θ_{m1}). We are therefore able to study the reaction mechanisms dominating various angular regions in the studied systems. For example, in Figure 3a,b we selected events where the largest fragment m_1 was emitted at very forward angles ($\Theta_{m1} \leq 10°$). In this angular region, the ΔM_{nor} spectra are peaked near 0.6 (a value associated typically to the production of evaporation residues), and the $^{40}Ca + ^{48}Ca$ system shows an higher probability of populating high values of ΔM_{nor} compared to the other two, more neutron poor, systems. In panels 4c,d, we selected events where the largest fragment was emitted at larger angles; in this case ΔM_{nor} distributions are clearly shifted to lower values. This is a clear signal that reaction mechanisms dominating this angular region are associated to the production of two or more fragments of similar masses.

From a qualitative point of view, the experimentally observed large probability of producing heavy residues in neutron-rich reactions could be related to their larger neutron content. Hot quasi-fused nuclei formed in this neutron rich system are pushed close to the stability valley. On the contrary intermediate systems formed with $N \simeq Z$ targets are much closer to the proton drip line and can be affected by Coulomb instabilities that unfavor the survival of evaporation residues at high excitation energies [19]. In order to investigate in more details the role played by Coulomb and Symmetry terms in the evolution of collision dynamics, we compared experimental results concerning ΔM_{nor} distributions with Constrained Molecular Dynamics model predictions [9, 12, 13]. Calculations have been performed by adopting different options for the stiffness of the symmetry energy. As shown in [9], a nice reproduction of experimental data is obtained when we parameterize the symmetry potential as a linear function of nuclear density.

4. Conclusions and perspectives

We investigated effects of the neutron to proton ratio on the collision dynamics of nuclear reactions involving (mainly) calcium beams and targets at 25 MeV/nucleon. It seems that the competition between various reaction scenarios present at semi-central impact parameters (evaporation residue versus two or more fragments emission) is highly sensitive to the neutron richness of the entrance channel. Mass selections and angular distributions of the two largest fragments emitted allow to disentangle better the balance between various reaction mechanisms observed.

Comparisons of experimental data with Constrained Molecular Dynamics model calculations allowed to obtain information about the density dependent part of the symmetry potential of the Nuclear Equation of State. All these findings open the way for further investigations that can be performed by using radioactive (proton rich and neutron rich) ion beams, in order to enlarge the available systematics of experimental data to very far from stability systems. In this way, effects due to the neutron to proton ratio degree of freedom can be enhanced and further details about the behavior of symmetry energy could be obtained.

Thanks are due to Dr. D. Rifuggiato and INFN-LNS accelerator staff for delivering beams of very good timing properties. We acknowledge also C.Marchetta and E.Costa for providing high quality Ca targets.

References

[1] Bao-An Li et al 2008, *Phys. Rep.* 464 113
[2] V. Baran et al 2005, *Phys. Rep.* 410 335
[3] S. Kumar et al 2010, *Phys. Rev.* C 81 014611
[4] M.B. Tsang et al 2009, *Phys. Rev. Lett.* 102 122701
[5] M. Colonna et al 1998, *Phys. Rev.* C 57 1410
[6] L. Shvedov et al 2010, *Phys. Rev.* C 81 054605
[7] W. Rosch et al 1990, *Nucl. Phys.* A 509 615
[8] B. Jakobsson et al 1990, *Nucl. Phys.* A 509 195
[9] F. Amorini et al 2009, *Phys. Rev. Lett.* 102 112701
[10] I. Lombardo et al 2010, *Nucl. Phys.* A 834 458
[11] I. Lombardo et al 2011, *Acta Phys. Pol.* B 42 701
[12] M. Papa et al 2001, *Phys. Rev.* C 64 024612
[13] M. Papa and G. Giuliani 2009, *Eur. Phys. Jour.* A 39 117
[14] A. Pagano et al 2004, *Nucl. Phys.* A 734 504
[15] N. Le Neindre et al 2002, *Nucl. Instrum. Methods* A 490 251
[16] M. Alderighi et al 2002, *Nucl. Instrum. Methods* A 489 257
[17] C. Cavata et al 1990, *Phys. Rev.* C 42 1760
[18] H.-J. Keim et al 1987, *Zeit. Phys.* A 327 101
[19] J. Besprosvany and S. Levit 1989, *Phys. Lett.* B 217 1